

Rapid Communications

Rapid Communications are intended for the accelerated publication of important new results and are therefore given priority treatment both in the editorial office and in production. A Rapid Communication in Physical Review B should be no longer than four printed pages and must be accompanied by an abstract. Page proofs are sent to authors.

Charge-density-wave structure and a metal-insulator transition in Cr_xNbSe_3 detected by atomic force microscopy and transport measurements

Q. Xue, Z. Dai, Y. Gong, C. G. Slough, and R. V. Coleman

Physics Department, University of Virginia, Charlottesville, Virginia 22901

(Received 11 March 1993)

The addition of Cr to NbSe_3 at low concentrations reduces the charge-density-wave energy gaps and modifies the Fermi surface. As the concentration is increased to 5 at. % a new phase exhibiting a metal-insulator transition at ~ 700 K is formed. Atomic force microscopy shows a strong static charge modulation with a wavelength of three times the atomic spacing and the crystal is completely insulating at room temperature.

The addition of Cr to NbSe_3 produces a number of phases having different linear chain structures and unusual electronic properties. Previous studies of $\text{Cr}_{0.67}\text{NbSe}_3$ by Ben Salem *et al.*¹ and Cava *et al.*² showed that it formed a new linear chain structure of the form $\text{Cr}_{1.6}\text{Nb}_{2.4}\text{Se}_{10}$ with four chains per unit cell rather than six as found in pure NbSe_3 . This new phase showed a metal-insulator transition with an onset temperature of ~ 140 K similar to that previously observed by Hillenius *et al.*³ in $\text{Fe}_{0.25}\text{Nb}_{0.75}\text{Se}_3$. This latter compound also formed a structure with four chains per unit cell of the form $\text{FeNb}_3\text{Se}_{10}$. Hillenius *et al.*³ also showed that the metal-insulator transition was induced by a charge-density wave (CDW).

In this paper we report the discovery of a dilute Cr-doped phase of NbSe_3 that exhibits a metal-insulator transition at a much higher temperature with an onset temperature of ~ 700 K. Atomic force microscopy (AFM) scans on this new phase also indicate a very strong charge modulation along the chains with a wavelength equal to approximately three atomic spacings. At Cr concentrations in the range $x=0-0.04$, Cr_xNbSe_3 is only slightly changed in structure from that of pure NbSe_3 . The normal Fermi surface pocket is modified and the CDW gaps are reduced, but the two CDW transitions as observed in the resistance versus temperature show relatively small changes in the onset temperatures. As shown in Fig. 1 for $\text{Cr}_{0.03}\text{NbSe}_3$, the two resistance anomalies associated with the CDW's are still strong with onset temperatures that are reduced from 144 to 140 K for T_2 and 59 to 56 K for T_1 . As shown in Fig. 2 the CDW energy gaps are reduced from $\Delta_2=101.2\pm 1.8$ to 42.7 ± 3.2 meV and $\Delta_1=35.0\pm 1.3$ to 25.3 ± 3.7 meV, respectively, as measured by scanning tunneling micro-

scope (STM) spectroscopy. The extremal sections of the normal Fermi surface (FS) as measured for field directions lying in the *a-c* plane also become more isotropic as shown in Fig. 3. The frequency rises for field directions near the *c* axis while it decreases substantially for field directions near the CDW *q*-vector direction projected on the *a-c* plane. This indicates a considerable change in the anisotropy of the CDW energy gaps, although the energy gaps measured in Fig. 2 are for tunneling only in the direction perpendicular to the *c* axis. However, the large changes in the measured CDW energy gaps are consistent with the substantial change observed in the normal FS anisotropy. AFM scans of $\text{Cr}_{0.03}\text{NbSe}_3$ at room temperature show three chains per unit surface cell as shown in Fig. 4. One chain is high and two are low consistent with

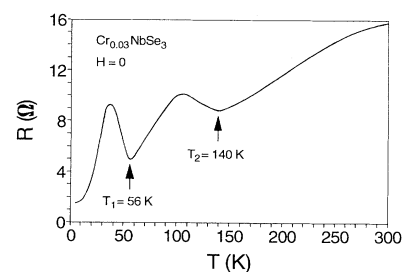


FIG. 1. Temperature dependence of resistance along the *b* axis for $\text{Cr}_{0.03}\text{NbSe}_3$. The two CDW phase transitions are characterized by giant resistance anomalies with onsets at $T_1=56$ K and $T_2=140$ K. Both are reduced compared to $T_1=59$ K and $T_2=144$ K observed for pure NbSe_3 . The overall shape of the curve is very similar to that observed for pure NbSe_3 .

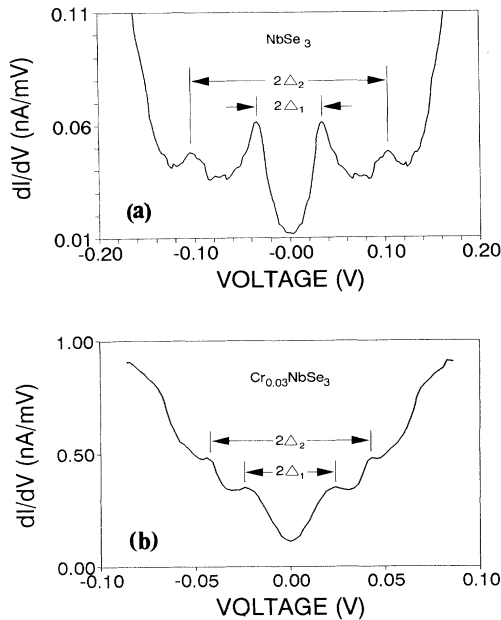


FIG. 2. Conductance vs bias-voltage curves measured at 4.2 K for pure NbSe_3 and $\text{Cr}_{0.03}\text{NbSe}_3$. The arrows indicate the CDW gap edges. (a) Pure NbSe_3 exhibits CDW gap edges at ± 101.2 and ± 35.0 mV. (b) $\text{Cr}_{0.03}\text{NbSe}_3$ exhibits CDW gap edges at ± 42.7 and ± 25.3 mV. These are reduced by $\sim 60\%$ and $\sim 30\%$, respectively, compared to those observed in pure NbSe_3 .

the chain structure observed for pure NbSe_3 . However, there is a weak charge modulation of $\sim 2b_0$ along the chains induced by the presence of Cr which at these dilute concentrations is likely to be located in the van der Waals gap below the surface unit cell. Charge transfer

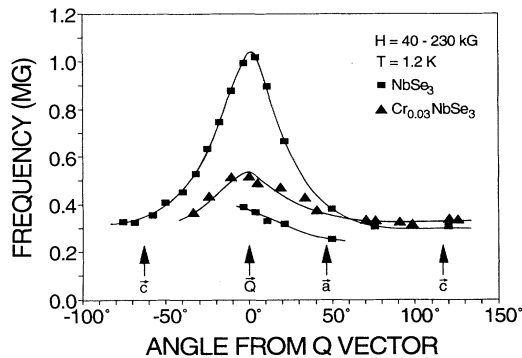


FIG. 3. Angular dependence of the quantum oscillation frequencies observed at 1.2 K in NbSe_3 (solid rectangles) and $\text{Cr}_{0.03}\text{NbSe}_3$ (solid triangles) for magnetic fields lying in the \mathbf{a} - \mathbf{c} plane. Each curve shows a maximum near the direction \mathbf{Q} which represents the low-temperature CDW \mathbf{q} -vector direction projected on the \mathbf{a} - \mathbf{c} plane. The frequency of $\text{Cr}_{0.03}\text{NbSe}_3$ rises for magnetic-field directions near the \mathbf{c} axis while it decreases significantly for magnetic-field directions near the \mathbf{Q} -vector direction compared to the frequencies observed for pure NbSe_3 . An additional low-frequency branch is observed for pure NbSe_3 .

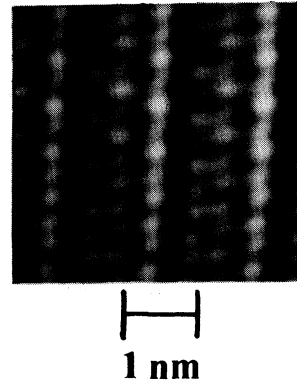


FIG. 4. AFM scan at room temperature on $\text{Cr}_{0.03}\text{NbSe}_3$ recorded in the constant force mode. The crystal structure observed is consistent with that for pure NbSe_3 with one high chain and two low chains. However, the image indicates a weak charge modulation of $2b_0$ along the chains induced by the presence of the dilute concentration of Cr.

from the Cr can occur as is also observed in the layer dichalcogenides⁴ where ordered superlattices of Fe in the van der Waals gap create substantial charge transfer to the surface Se atoms.

For $x = 0.05$ the crystal structure shows an abrupt change and becomes insulating at room temperature. Scans with the atomic force microscope show a large modulation of the static charge at a wavelength of approximately 3 atomic spacings as shown in Fig. 5. Figure 5(a) shows both the atomic modulation and the charge modulation, while Fig. 5(b) shows only the charge modulation. Each chain appears to be identical except for the phase displacement of the charge modulation on adjacent chains. This phase displacement is $\sim 120^\circ$ and indicates three surface chains per unit cell for the superlattice.

The insulating state and the strong charge modulation appear to be connected with a metal-insulator transition with an onset above ~ 700 K as shown in the resistance versus temperature curve of Fig. 6. The resistance has risen to $10 \text{ M}\Omega$ at 620 K and rises to an insulating state in the lower temperature range. The initial rise in resistance is similar to that observed in $\text{FeNb}_3\text{Se}_{10}$ or $\text{Cr}_{1.6}\text{Nb}_{2.4}\text{Se}_{10}$, but neither of these compounds becomes insulating even at helium temperatures.^{2,3} STM tunneling into $\text{Cr}_{0.05}\text{NbSe}_3$ is not possible at room temperature for bias voltages up to 10 V, while $\text{FeNb}_3\text{Se}_{10}$ shows tunneling at 4.2 K at relatively low bias voltages.

In $\text{Cr}_{0.05}\text{NbSe}_3$ the strong charge modulation and the insulating state may be connected with a commensurate structure. In $\text{FeNb}_3\text{Se}_{10}$ the metal-insulator transition is induced by a CDW, but it remains incommensurate³ down to 6 K. Although the onset and resistance rise in $\text{Cr}_{0.05}\text{NbSe}_3$ is very similar, the abrupt rise below 600 K may be connected with an incommensurate to commensurate transition. X-ray diffraction work to determine the crystal structure and to detect the possible CDW structure is planned, but larger crystals are required and are

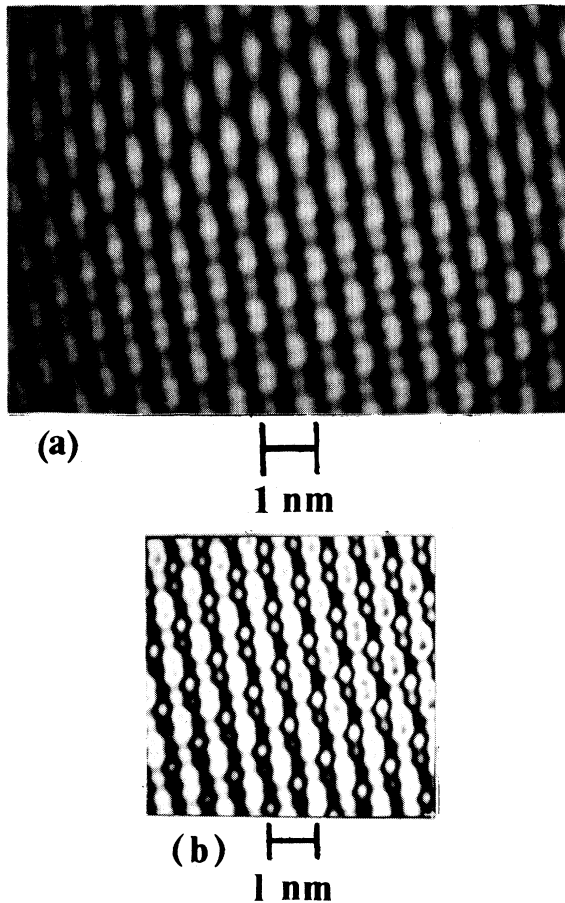


FIG. 5. (a) AFM scan at room temperature on $\text{Cr}_{0.05}\text{NbSe}_3$ recorded in the constant force mode. The image shows a large charge modulation along the b axis at a wavelength of approximately 3 atomic spacings. Each chain appears identical except for a phase displacement of 120° for the charge maxima on adjacent chains. This indicates three surface chains per unit cell for the superlattice. The chain spacing is 6.5 \AA . (b) AFM scan at room temperature on the same crystal as in (a). The charge modulation of approximately 3 atomic spacings is detected both on the surface chains (continuous white areas) and between the surface chains (continuous black areas). For this adjustment of the look-up table two atoms are resolved along the chains below the surface, but the charge modulation remains at approximately three times the atomic spacing.

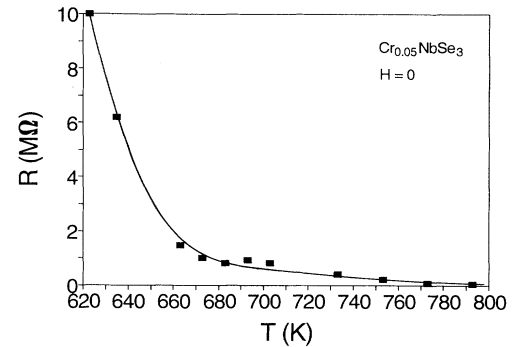


FIG. 6. Temperature dependence of resistance measured from 800 to 620 K for $\text{Cr}_{0.05}\text{NbSe}_3$. A strong metal-insulator transition is observed with an onset of $\sim 700 \text{ K}$. At 620 K the resistance reaches $10 \text{ M}\Omega$ while below 620 K the crystal rapidly becomes insulating.

currently being grown. The effect of dilute impurities on CDW pinning and quantum oscillations has been discussed by Coleman *et al.*⁵ in terms of magnetic breakdown of the CDW energy gaps. The role of the electronic modifications of the CDW by impurities and how they drive the phase transition need further study.

The high temperature at which this metal-insulator transition occurs and the fact that it proceeds to a complete insulating state make this material unique. Further studies to understand the mechanism should be interesting.

The authors wish to thank Professor L. M. Falicov for many stimulating discussions. Professor Robb Thorne provided the high-purity NbSe_3 crystal used for quantum oscillation measurements in pure NbSe_3 . The authors wish to thank Larry Rubin for much help and advice on the high magnetic-field experiments and W. W. McNairy for help with the crystal growth program. This research was partially supported by Department of Energy Grant No. DE-FG05-84ER4507 and National Science Foundation Grant No. DMR-8912694. The work in magnetic fields up to 230 kG was performed at the Francis Bitter National Magnet Laboratory, supported at the Massachusetts Institute of Technology by the National Science Foundation.

¹A. Ben Salem, A. Meerschaut, H. Salva, Z. Z. Wang, and T. Sambongi, *J. Phys. Paris* **45**, 771 (1984).

²R. J. Cava, F. J. DiSalvo, M. Eibschutz, and J. V. Waszczak, *Phys. Rev. B* **27**, 7412 (1983).

³S. J. Hillenius, R. V. Coleman, R. M. Fleming, and R. J. Cava,

Phys. Rev. B **23**, 1567 (1981).

⁴Z. Dai, Q. Xue, Y. Gong, C. G. Slough, and R. V. Coleman (unpublished).

⁵R. V. Coleman, M. P. Everson, Hao-An Lu, A. Johnson, and L. M. Falicov, *Phys. Rev. B* **41**, 460 (1990).

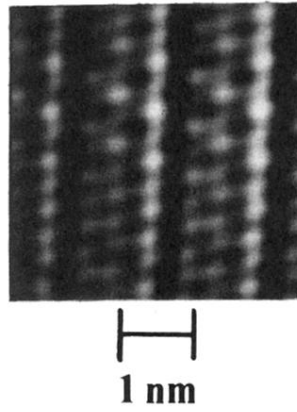


FIG. 4. AFM scan at room temperature on $\text{Cr}_{0.03}\text{NbSe}_3$ recorded in the constant force mode. The crystal structure observed is consistent with that for pure NbSe_3 with one high chain and two low chains. However, the image indicates a weak charge modulation of $2b_0$ along the chains induced by the presence of the dilute concentration of Cr.

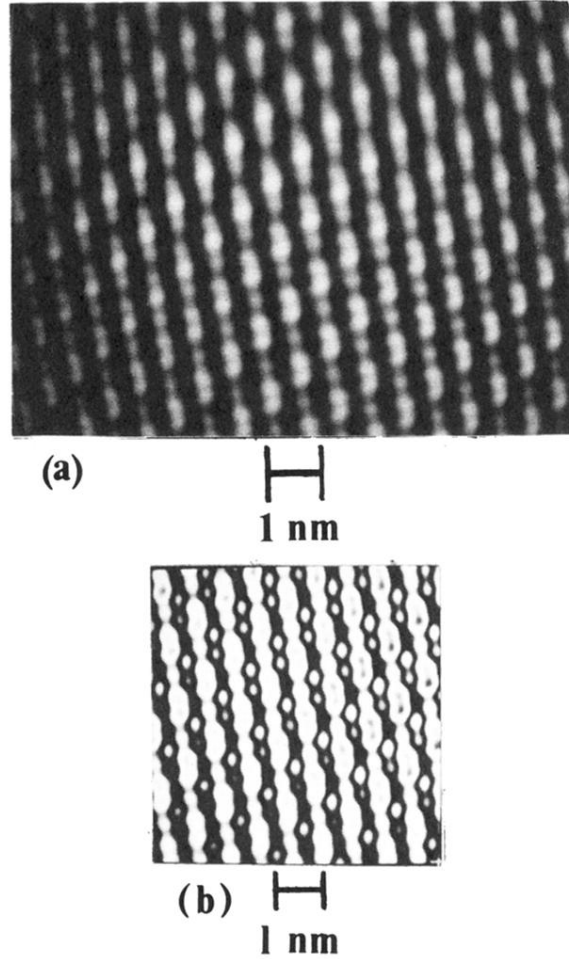


FIG. 5. (a) AFM scan at room temperature on $\text{Cr}_{0.05}\text{NbSe}_3$ recorded in the constant force mode. The image shows a large charge modulation along the \mathbf{b} axis at a wavelength of approximately 3 atomic spacings. Each chain appears identical except for a phase displacement of 120° for the charge maxima on adjacent chains. This indicates three surface chains per unit cell for the superlattice. The chain spacing is 6.5 \AA . (b) AFM scan at room temperature on the same crystal as in (a). The charge modulation of approximately 3 atomic spacings is detected both on the surface chains (continuous white areas) and between the surface chains (continuous black areas). For this adjustment of the look-up table two atoms are resolved along the chains below the surface, but the charge modulation remains at approximately three times the atomic spacing.